Revista Geoaraguaia
ISSN:2236-9716
Barra do Garças – MT
v.10, n. esp. Geologia e
Pedologia p. 80-107. Dez-2020

MINERAL CHEMISTRY AND GEOCHEMISTRY OF GRANITOID ROCKS IN NORTHERN OF SARDUIEH (DASHT SHAGHIN AND SARTASHTAK), IRAN

QUÍMICA MINERAL E GEOQUÍMICA DE ROCHAS GRANITÓIDES NO NORTE DE SARDUIEH (DASHT SHAGHIN E SARTASHTAK), IRÃ

Elahe Hosseini Nasab[1]

Mohamad Hashem Emami*[2]

Mansour Vosoughi Abedini[3]

Gholamreza Tajbakhsh[4]

Seyed Jamal Sheikh Zakariaee[5]

ABSTRACT

Dehaj-Sarduieh volcano-plutonic belt in Kerman province of Iran represents a part of Urumieh-Dokhtar Magmatic assemblage which is mainly composed of granodiorite, quartz diorite, tonalite granite and granophyre. These rocks emplaced in Eocene volcanic and pyroclastic deposits rocks and are considered to be Oligo-Miocene in age. Geochemical studies showed that the amphibole minerals in diorite and granodiorites are calcic in composition and range from actinolite to magnesio-hornblende. Geochemical and mineralogical results revealed that these bodies have been generated in the lower part of the lower crust at a temperature of 700 to 750 °C, with an oxygen fugacity of -13.57 to -15.76 and a low pressure of 1 to 3 kb through mixing of mantle-derived mafic magma with crustal-derived felsic melts. These amphiboles are subduction-related and in accordance with the tectono-magmatic features suggested for these massifs, they show the characteristics of subduction and active continental margin environments. Field observations and mineralogical-geochemical evidence revealed that the original magma has been calc-alkaline in composition and metaluminous I-type. It is also showed that the process of fractional

[1]Department of Geology, Science and Research Branch, Islamic Azad University, Tehran, Iran. elahe.hosseininasab@gmail.com ORCID: https://orcid.org/0000-0002-4833-4603

[2]Department of Geology, Islamshahr Branch, Islamic Azad University, Tehran, Iran. *Corresspounding author. hashememami@yahoo.com ORCID: https://orcid.org/0000-0002-3215-4237

[3] Department of Geology, Science and Research Branch, Islamic Azad University, Tehran, Iran. m.vossoughi16@yahoo.com ORCID: https://orcid.org/0000-0001-6818-4633

[4]Department of Geology, Yazd University, Yazd, Iran. grttajbakhsh@yahoo.com ORCID: https://orcid.org/0000-0002-1159-5471.

[5] Department of Geology, Science and Research Branch, Islamic Azad University, Tehran, Iran. jamal.zakariaee@gmail.com ORCID: https://orcid.org/0000-0003-4459-4886

Revista Geoaraguaia
ISSN:2236-9716
Barra do Garças – MT
v.10, n. esp. Geologia e
Pedologia p. 80-107. Dez-2020

crystallization has significantly contributed in the formation of these rocks. Sarduieh igneous rocks displayed an enrichment in the large-ion lithophile elements (LILE, e.g. Ce, Th, Ba, Zr, Sr) and a depletion of the high field strength elements (HFSE, e.g. Nb, P, and Ti) and Chondrite normalized REE patterns are characterized by LREE enrichment and Show slight negative Eu anomalies which reflect the influence of subductions zone and active continental margin environments. The tectonic setting of these rocks is inferred to be continental arc or active continental margin and they were deduced to be generated by the subduction of the Neotethys oceanic crust beneath the Central Iranian continental plate.
Keywords: Mineral chemistry; Geochemistry; Granitoid rocks; Sarduieh; Iran.

RESUMO

O cinturão vulcânico-plutônico de Dehaj-Sarduieh, na província de Kerman, no Irã, representa uma parte do conjunto Urumieh-Dokhtar Magmatic, composto principalmente de granodiorito, diorito de quartzo, granito e granito. Essas rochas localizadas em depósitos vulcânicos e piroclásticos do Eoceno e são consideradas como idade do Oligo-Mioceno. Estudos geoquímicos mostraram que os minerais anfibólio nos dioritos e granodioritos são de composição cálica e variam de actinolita a magnésio-hornblenda.Resultados geoquímicos e mineralógicos revelaram que esses corpos foram gerados na parte inferior da crosta inferior a uma temperatura de 700 a 750 ° C, com uma fugacidade de oxigênio de -13,57 a -15,76 e baixa pressão de 1 a 3 kb através da mistura de magma máfico derivado do manto com derretidos félsicos derivados da crosta. Esses anfibólios estão relacionados à subducção e, de acordo com as características tectono-magmáticas sugeridas para esses maciços, mostram as características dos ambientes de subducção e margem continental ativa. As observações de campo e as evidências mineralógico-geoquímicas revelaram que o magma original tem composição alcalino-calcária e tipo I metaluminoso. Também é mostrado que o processo de cristalização fracionada contribuiu significativamente na formação dessas rochas. As rochas ígneas de Sarduieh exibiram um enriquecimento nos elementos litófilos de íons grandes (LILE, por exemplo, Ce, Th, Ba, Zr, Sr) e um esgotamento dos elementos de alta força de campo (HFSE, por exemplo, Nb, P e Ti) e Condrita normalizados Os padrões REE são caracterizados pelo enriquecimento LREE e Mostrar pequenas anomalias negativas da Eu que refletem a influência da zona de subducção e ambientes ativos de margens continentais. O cenário tectônico dessas rochas é inferido como arco continental ou margem continental ativa e elas foram deduzidas para serem geradas pela subducção da crosta oceânica de Neotethys sob a placa continental iraniana central.
Palavras-chave: Química mineral; Geoquímica; Rochas granitóides; Sarduieh; Irã.

INTRODUCTION

Revista Geoaraguaia
ISSN:2236-9716
Barra do Garças – MT
v.10, n. esp. Geologia e
Pedologia p. 80-107. Dez-2020

Magmatic activity during the Cenozoic is one of the most significant igneous activities in Iran and has developed various features throughout the country. This volcanic phase has started from Eocene and continued to Pliocene and Quaternary times (Dilek, Sandvol, 2009) resulted in the formation of the Urumieh-Dokhtar Magmatic Arc (UDMA). The UDMA, with a NW-SE trend, extends along the active margin of the Central Iranian plate, between the Sanandaj-Sirjan and the Central Iran structural zones (Figure 1). The UDMA is a segment of Alpine-Himalayan Belt (Berberian, King, 1981) and the thickness of its intrusive and extrusive rocks reaches a maximum of 4 km (Alavi, 1994). This magmatic activity started during the Eocene and has been active until today (Berberian *et al.*, 1982; Berberian, King, 1981). Dehaj-Sarduieh volcano-plutonic belt in Central Iran, represents the largest volume of magmatic rocks in the UDMA (Berberian *et al.*, 1982). There is no consensus on the origin of the plutonic and volcanic rocks in the UDMA though the following geodynamic models have been suggested: (i) some researchers believe that the UDMA has been formed as a result of the subduction of Neotethys oceanic slab beneath the Central Iranian Plate (Aftabi, Atapour 2000; Berberian, King, 1981; Moïne-Vaziri, 1985; Nowroozi, 1971; Takin, 1972), (ii) some scholars attributed the UDMA to the subduction of the Arabian plate under the Eurasian plate (Agard *et al.*, 2005; Agard *et al.*, 2011; Dilek *et al.*, 2009; Ghasemi, Talbot, 2006), (iii) according to many scientists (Amidi, 1977; Caillat *et al.*, 1978; Emami, 1981; Lescuyer, Riou, 1976; Sabzehei *et al.*, 1994) the formation of the UDMA is related to the magmatic in intra-continental rift setting, (iv) some other researchers extended their idea and suggest that the UDMA has developed in a vast magmatic province during the convergence between the AfroArabian and Eurasian plates (Allen *et al.*, 2004; Dewey *et al.*, 1989; Dilek, Sandvol, 2009; McClusky *et al.*, 2000) which has led to the dominance of volcanic rocks in north and northwest of Bitlis-Zagros suture zone (Dilek *et al.*, 2010). There is also a theory which considers both subduction and continental rift settings and the generation of a sub-alkaline melt through flux melting resulted from decompression melting during an oblique

Revista Geoaraguaia
ISSN:2236-9716
Barra do Garças – MT
v.10, n. esp. Geologia e
Pedologia p. 80-107. Dez-2020

subduction. In The study research granitoids of The North of Sarduieh (located in the Urumieh-Dokhtar Magmatic Arc (UDMA), Iran) has been investigated in terms of petrology, geochemistry and tectonic setting.

MATERIALS AND METHODS

After a reconnaissance and field observation, a number of 150 rock samples from various plutonic unites of Sarduieh were collected for petrographic and geochemical studies. The attempt was to collect the rocks from fresh, unweathered outcrops including diorite, tonalite, granodiorite, granite and granophyre. The thin sections of 100 rock samples were prepared at Shahid Bahonar University and the petrographic studies were conducted using polarized microscope at Islamic Azad University, Science and Research Branch, Tehran. Twenty-nine samples from unaltered rocks were selected for geochemical analyses. Samples were oven dried at 110 °C and then were ground and powdered to below 75 micron. They then were sent to ALS Geochemistry Analytical Lab, Canada for determining the content of major and trace elements by ICP-MS E81. The results were processed by GCDkit and Igpet softwares. The results of the geochemical analyses are shown in Table 1. Mineralogical composition of amphibole minerals in diorite and granodiorites was studied using electron microprobe analyzer with energy dispersive x-ray spectroscopy (EDX) at Kansaran Binaloud laboratory, Iran. The electron beam resolution of machine was 15NA at 20 kV (STEM).

RESAULT AND DISCUSSION

The study area is located in north of Sarduieh, Kerman province of Iran between the latitudes of 29° 22´-29° 24´N and the longitudes of 57° 13´- 57° 27´E (Figure 2). It is situated in the Urumieh-Dokhtar Magmatic Arc (UDMA) (Berberian 1983) and has been found to be a segment of Dehaj-Sarduieh volcano-plutonic belt in the southern part of the Sahand-Bazman Magmatic Arc. Plutonic rocks of Sarduieh are mainly from the Late Eocene to Oligo-Miocene epochs and are extended in NW- SE direction along the UDMA. Igneous rocks of Sarduieh are classified in three groups of volcanic and pyroclastic, sub-volcanic and plutonic

Revista Geoaraguaia
ISSN:2236-9716
Barra do Garças – MT
v.10, n. esp. Geologia e
Pedologia p. 80-107. Dez-2020

based on their petrology, age and mode of formation. The latter group rocks are intruded by younger dikes with a composition ranging from quartz diorite porphyry to andesite porphyry depends on the depth of cooling. The composition of Eocene pyroclastic volcanic rocks, with several thousand meters thickness, range from acidic to basic while the intermediate rocks of dacite andesite and andesite basalt are dominant. Sub-volcanic and plutonic rocks and Oligo-Miocene dikes are located in the southeast and are mainly comprised of granodiorite, quartzdiorite, granite and granophyre.

PETROGRAPHY

The petrographic study of the Sarduieh rock units showed that they are comprised of quartz diorite, tonalite, granodiorite, granite and granophyre.

QUARTZ DIORITE

These rocks are mainly composed of plagioclase and quartz and accessory minerals of alkali-feldspar, amphibole and opaque minerals. The rocks primarily show a granular texture. The presence of the small inclusions of apatite crystals in plagioclase and opaque minerals in amphibole has created a poikilitic texture (Figure 3a). Plagioclase phenocrysts with polysynthetic twinning and rarely with crystal zoning are disseminated in rocks. In some cases, plagioclase has been altered to clay minerals and sericite. The rocks contain anhedral to subhedral amphibole crystals which have been to some extent altered to chlorite. Quartz grains in small to medium sizes are crystallized and fill the void spaces between the minerals.

TONALITE

Tonalite is composed of plagioclase and quartz and in minor amounts of sphene, apatite, amphibole, alkali feldspar, biotite and opaque minerals. Tonalite shows granular texture (Figure 3b). Anhedral to subhedral phenocrysts of plagioclase with polysynthetic twinning and no crystal zoning occurred in the rocks which have been occasionally altered to clay minerals and sericite. Anhedral alkali-feldspar minerals in tonalites are filling the void spaces between the plagioclase grains and are generally altered to clay minerals. Euhedral

Revista Geoaraguaia
ISSN:2236-9716
Barra do Garças – MT
v.10, n. esp. Geologia e
Pedologia p. 80-107. Dez-2020

to anhedral grains of amphibole are present as inclusion in plagioclase and display an alteration to chlorite minerals. Small to medium-size anhedral quartz are filled the void spaces between the grains.

GRANODIORITE

Granodiorites contain plagioclase, amphibole and quartz with minor amounts of apatite, zircon and sphene, These rocks are granular and poikilitic in texture (Figure 3c). Plagioclase minerals are medium to coarse grained euhedral to subhedral andesine to labradorite with polysynthetic or albite twinning with oscillatory zoning, corroded rims and mesh texture. They display signs of alteration to chlorite minerals. Small to medium-size anhedral quartz are filled the empty spaces between the minerals.

GRANITE

Granites are composed of plagioclase, alkali-feldspar, amphibole and secondary minerals of chlorite, calcite and sphene. Accessory minerals of apatite, amphibole, biotite and opaque minerals are found in these rocks. The main texture of these rocks is granular but poikilitic texture is also observed (Figure 3d). The rocks contain euhedral to subhedral plagioclase with albite twinning and mesh texture. Similar to other rocks, plagioclase minerals in granites are to some extent altered to clay minerals and sericite. Alkali-feldspars are euhedral to subhedral and are relatively altered to clay minerals. Euhedral to subhedral amphibole microlites are enclosed by opaque minerals as inclusion and they have been altered to chlorite in some cases. Quartz in the form of anhedral mineral fills the open spaces in the rock.

GRANOPHYRE

Alkali-feldspar, quartz and plagioclase are the main mineral constituents of granophyres. Accessory minerals include amphibole, biotite, zircon, apatite and opaque minerals. These rocks show granophyric texture (Figure 3e) resulted from the intergrowth of quartz and anhedral alkali feldspar minerals. They show signs of alteration to clay minerals.

Plagioclase minerals are euhedral to subhedral oligoclase and present albite twinning. Some of the plagioclase minerals are altered to clay minerals and sericite.

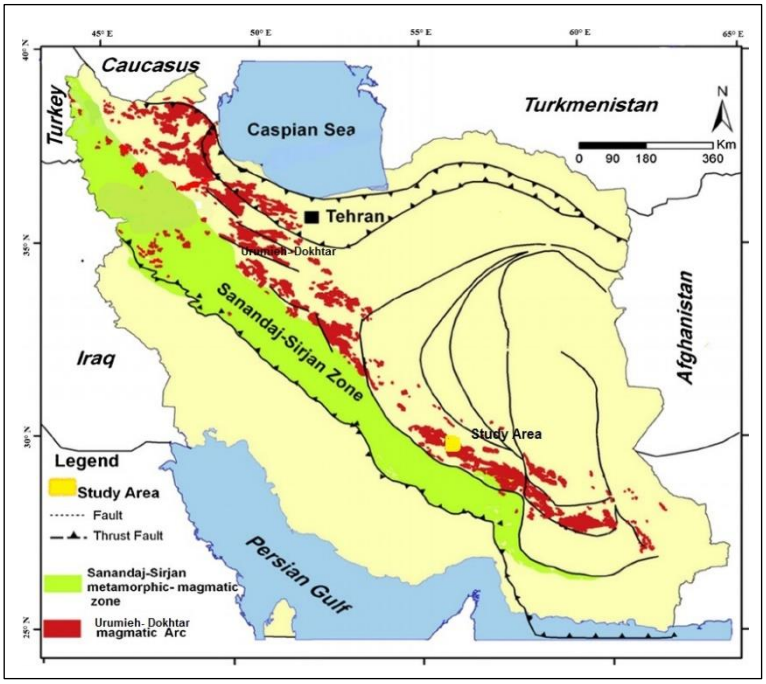

Figure 1. Map of structural zones of Iran showing the location of the study area in the UDMA. Source: Alavi, (1994)

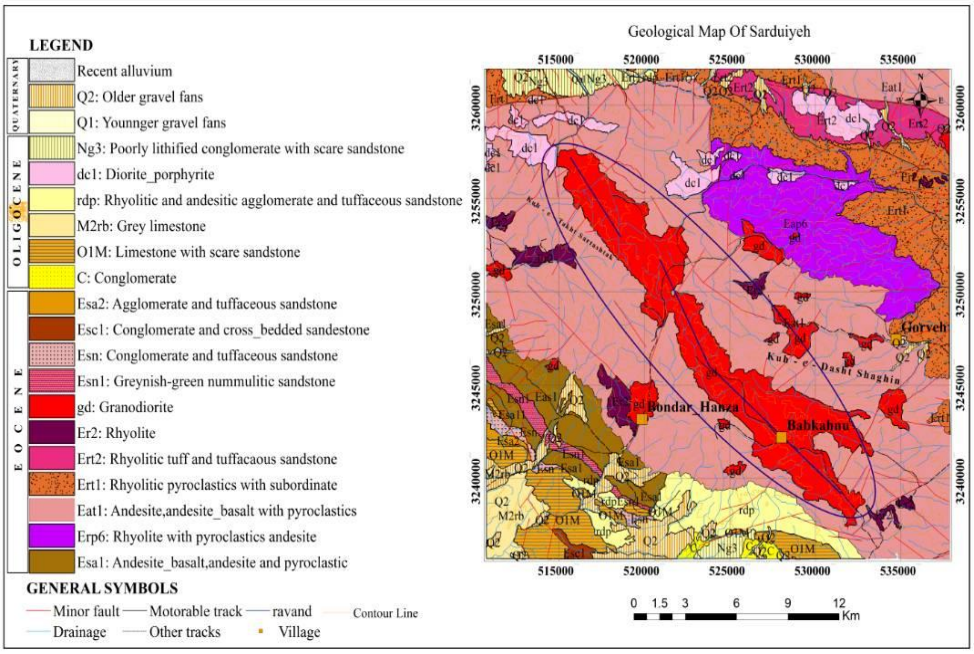

Figure 2. The location of the study area on geological map 1:100,000 of Sarduiyeh.

Source: GSI (1972).

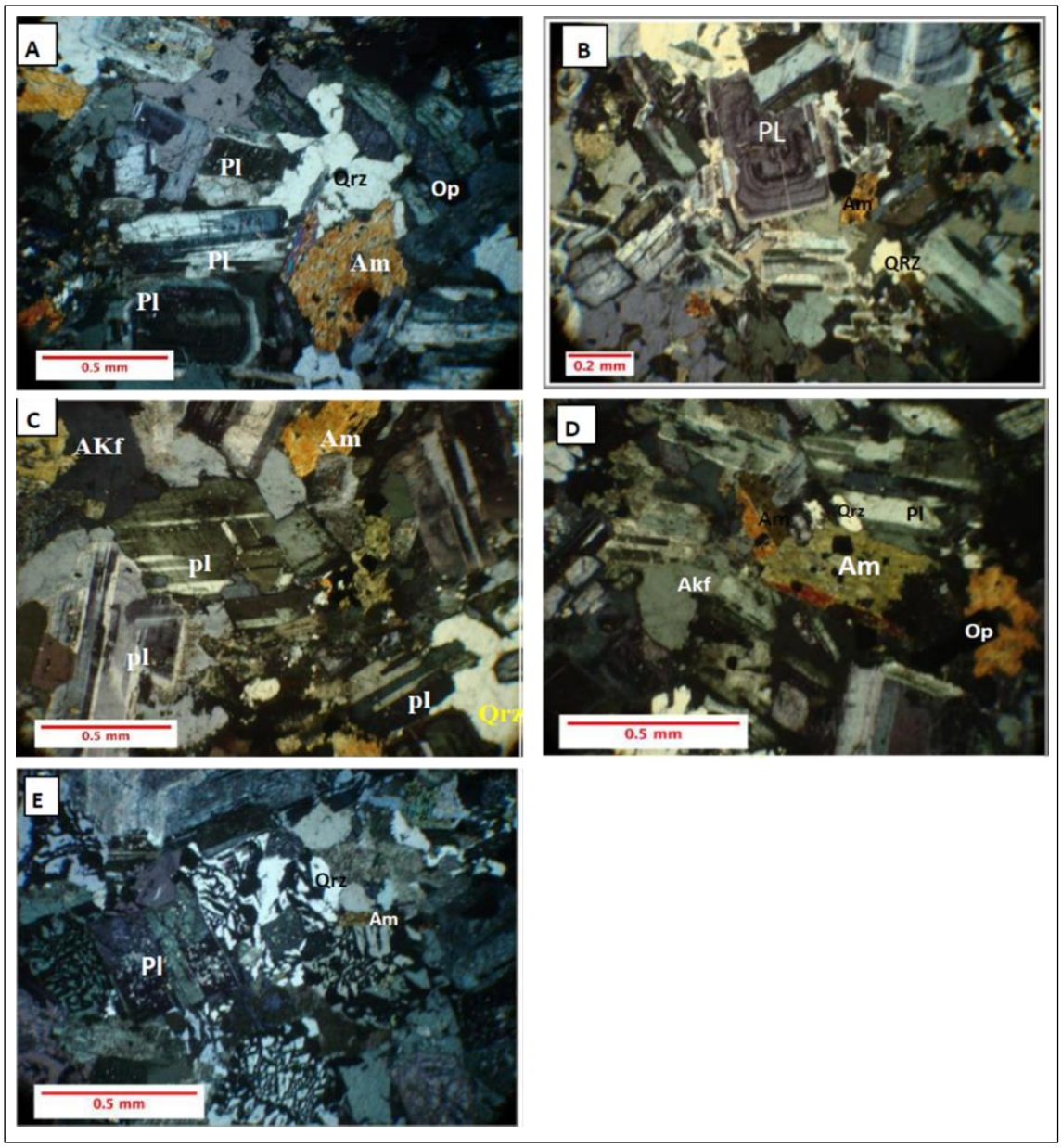

Figure 3. Photomicrograph of (*a*) plagioclase minerals showing polysynthetic twinning and zoning (in cross-polarized light; XPL); (*b*) plagioclase with polysynthetic twinning and zoning textures along with amphibole and anhedral quartz in tonalite (XPL); (*c*) plagioclase with polysynthetic twinning and pericline, amphibole, alkali-feldspar and quartz in granodiorite (XPL); (*d*) poikilitic texture,

alkali-feldspar and quartz in granite (XPL); (*e*) intergrowth of alkali-feldspar and quartz and plagioclase and amphibole minerals in granophyre (XPL).
The Source of PHD dissertatioz Elahe Hosseininasab 2018

CHEMICAL COMPOSITION OF AMPHIBOLE

Cation calculation was conducted on the basis of 23 oxygen atoms in the amphibole minerals in granodiorites and diorites. According to amphibole classification scheme proposed by Leake *et al.* (1997), the studied amphibole minerals are calcic and are classified as magnesio-hornblende and actinolite hornblende (Figure 4). The amphiboles that range from magnesio- hornblende in the center to actinolite toward the margin, reflect the changes in physico-chemical properties of magma at the last stages of crystallization (Celic and Delaloye, 2006). These fall in the field of igneous amphibole in the Sial *et al.* (1998) diagram which is used to distinguish igneous amphiboles from metamorphic ones (Figure 5a). Chemical composition of amphibole reveals the attributes of parent magma and hence can be used to recognize the type of magma (Molina *et al.*, 2009). In this study, the composition of amphiboles indicates a sub-alkaline parent magma. (Figure 5b).

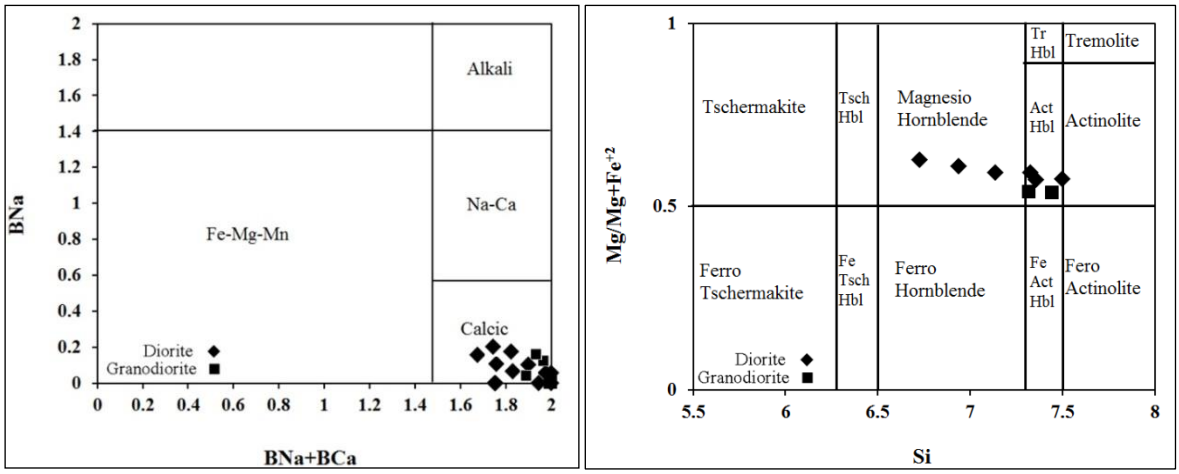

Figure 4. Chemical composition of amphiboles in diorites and granodiorites classification. Source: Leake *et al.* (1997).

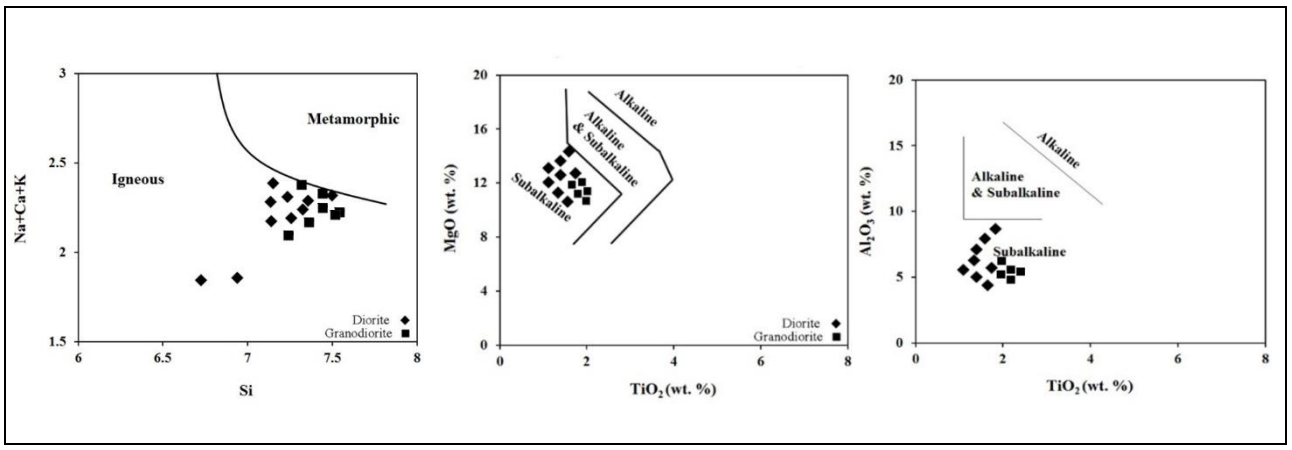

Figure 5. (*a*) TiO_2 vs. Al_2O_3 discriminant diagram to differentiate igneous amphibole frommetamorphic amphibole; (*b*) TiO_2 ,Al_2O_3versus Na_2O discriminant diagram to distinguish the nature of magma based on the composition of amphibole minerals in diorite and granodiorite. Source: Sial *et al.* (1998); Molina *et al.* (2009).

GEOBAROMETRY, OXYGEN FUGACITY, GEOTHERMOMETRY

According to Anderson (1983), the content of Ti in hornblende increases by temperature. Using the variation ratio of Ti versus Al per formula unit of amphibole, Helz (1993) has evaluated the temperature of formation of this mineral. The Ti versus AlIV variation suggests a temperature of 700 to 750 °C for crystallization of amphibole in diorites (Figure 6a). There is a positive correlation between Alt and AlIV and thus the method after Hammarstrom and Zen (1986) can be used for geobarometry of granitoids (Figure 6b). Variation in the composition of amphiboles is due to the changes in. At the time of formation of the granitoids in the region, the low oxygen fugacity of -13.57 to -15.76 is proposed which is intermediate according to the Anderson and Smith (1983) classification for amphiboles (Figure 6b).

$$\log fO2 = -30930/T + 14.98 + 0.142(P-1)/T$$

The content of Al in hornblende was used to evaluate the pressure at the zone of formation of igneous rocks in the region. Based on the total Al against Fe/(Fe+Mg) diagram (Schmidt, 1992), a pressure range of 1 to 3 kbar is suggested for the amphibole minerals in

diorites (Figure 11). The amount of Al in the hornblendes has a linear relationship with the crystallization pressure (Vyhnal *et al.*, 199). There is a correlation between Alt and AlIV in amphiboles and thus the method proposed by Hammarstrom and Zen (1986) can be used for geobarometry of granitoids.

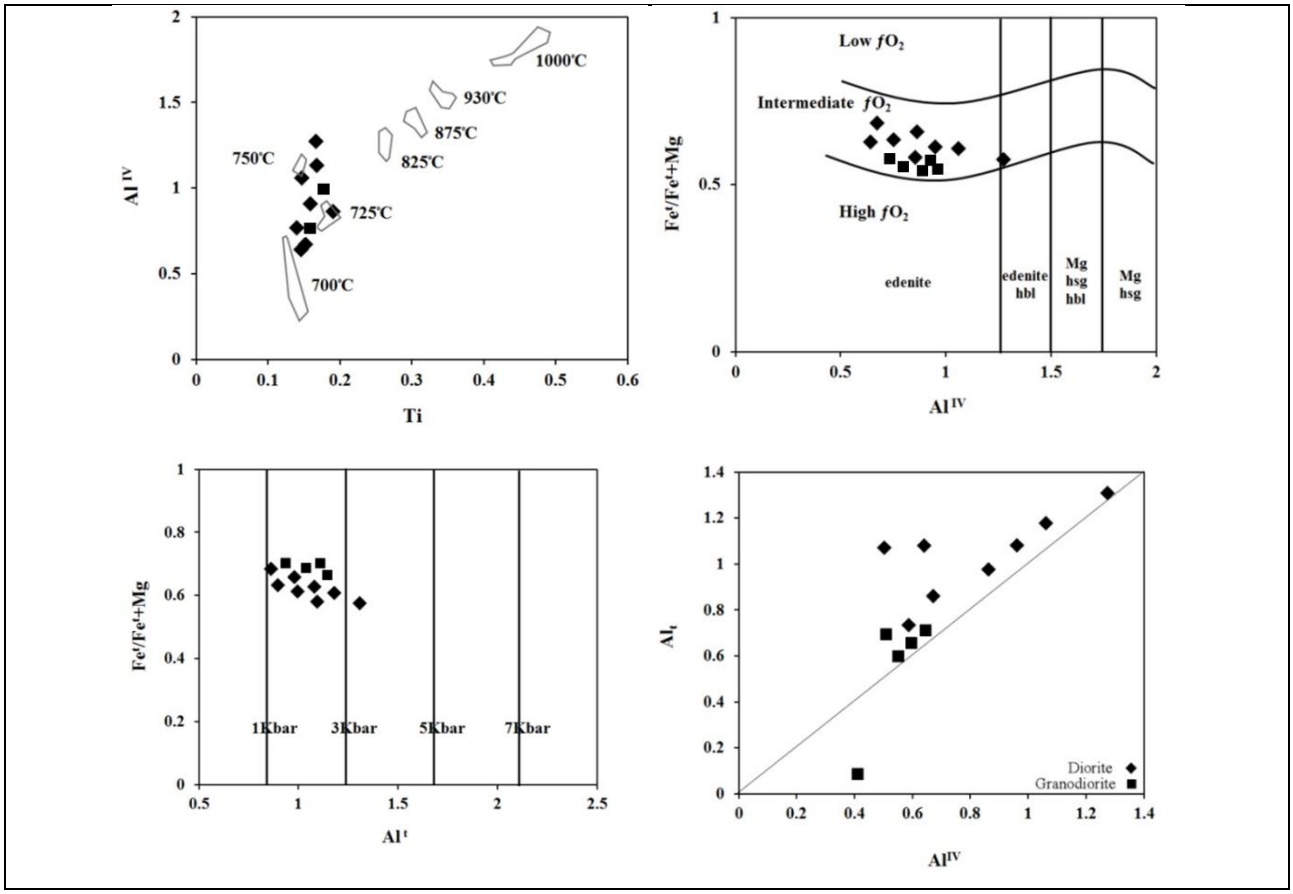

Figure 6. (*a*) Relative temperature of crystallization of the amphiboles in diorites and granodiorite; (*b*) Oxygen fugacity diagram on the basis of the composition of the amphiboles in diorites and granodiorite; (*c*) Al^T vs. Fe/(Fe+Mg) diagram indicating the pressure of crystallization of amphibole minerals in diorite and granodiorite; (*d*) Linear relationship between Al^t and Al^{IV} in amphibole minerals in diorite and granodiorite.

Source: Helz, (1973); Anderson and Smith (1995); Schmid, (1992).

Point	**Diorite**						
	E1	E2	E3	E3	E4	E9	E6
SiO2	51.89	49.91	48.36	4.42	48.24	47.66	47.54
TiO2	0.25	0.88	1.24	1.27	1.29	1.62	1.67
Al2O3	2.72	4.78	5.55	6.07	6.00	6.76	7.03
FeO	18.31	13.87	13.99	1.84	13.79	13.82	13.76

Revista Geoaraguaia
ISSN:2236-9716
Barra do Garças – MT
v.10, n. esp. Geologia e
Pedologia p. 80-107. Dez-2020

Point	**Diorite**						
	E1	E2	E3	E3	E4	E9	E6
MgO	17.44	15.99	15	1.02	14.99	14.72	14.67
MnO	0.93	0.42	0.34	0.39	0.38	0.32	0.32
CaO	5.54	10.78	11.11	1.99	10.97	11	11.05
Na2O	0.41	0.8	1.14	1.14	1.5	1.65	1.55
K2O	0.18	0.54	0.58	0.47	0.56	0.55	0.54
Sum	97.67	97.06	97.31	9.61	97.72	96.10	98.13
Si	7.53	7.206	7.07	0.25	7.02	6.913	6.88
Aliv	0.46	0.79	0.92	0.97	0.97	1.087	1.11
Altotal	0.46	0.81	0.95	0.38	1.03	1.15	1.2
T	8	8	8	8	8	8	8
Alvi	0.00	0.02	0.03	0.06	0.05	0.06	0.08
Ti	0.02	0.09	0.136	0.139	0.141	0.177	0.182
Fe+3	0.26	0.33	0.31	0.45	0.32	0.39	0.45
Mg	3.77	3.44	3.27	0.24	3.25	3.182	3.16
Mn	0.11	00.5	0.042	0.04	0.04	0.03	0.03
Fe+2	0.82	1.60	1.20	0.44	1.17	1.141	1.083
Ca	0.00	0.00	0.00	0.00	0.00	0.00	0.00
C	5	5	5	5	5	5	5
Fe	1.13	0.28	0.195	0.17	0.179	0.14	0.131
Ca	0.86	1.68	1.74	0.78	1.712	1.71	1.714
Na	0	0.03	0.06	0.11	0.1	0.146	0.155
B	2	2	2	2	2	2	2
Ca	0	0	0	0	0	0	0
Na	0.11	0.18	0.26	0.2	0.315	0.318	0.28
K	0.03	0.09	0.108	0.28	0.10	0.10	0.1
Sum A	0.149	0.278	0.369	0.292	0.419	0.419	0.379
Sum cations	14.14	15.28	15.36	1.29	15.41	15.41	15.37

Table 1. Results of microprobe mineralization in diorite based on 23 structural oxygen. Source: Kansaran Binaloud Institute of Iran

point	E1m50	E2m50	E1m53	E2m53	E3m53	E4m53	E1m20	E2m20	E3m20	E3m20
SiO2	49.7	50.09	66.46	58.49	49.81	48.98	50.81	49.15	48.91	49.14
TiO2	1.26	0.96	1.07	1.25	1.22	1.36	1.05	1.3	1.36	1.34
Al2O3	5.03	4.72	5.61	5.88	5.27	5.89	5.46	5.43	5.83	5.71
FeO	11.5	12.42	12.56	12.67	12.07	12.25	12.09	11.85	12.14	12.82
MgO	16.07	24.15	15.37	15.27	15.7	15.22	15.8	15.09	15.53	15.5
MnO	0.35	0.4	0.36	0.35	0.32	0.3	0.3	0.3	0.3	0.3
CaO	11.53	11.53	11.35	11.6	11.45	11.36	11.42	11.44	11.5	11.43
Na2O	1.31	1.44	1.28	1.27	1.29	1.47	1.15	1.5	1.53	1.6
K2O	1.55	1.64	1.51	1.48	0.31	0.35	0.33	0.75	0.52	0.54
Sum	97.38	96.10	97.77	98.35	97.44	97.18	98.43	96.86	97.62	97.65
Si	7.193	7.2	7.1	7.09	7.17	7.08	7.22	7.15	7.07	7.18
Aliv	0.807	0.73	0.86	0.90	0.82	0.91	0.77	0.84	0.93	0.94
Altotal	0.85	0.80	0.95	0.99	0.89	1.0	0.9	0.93	0.99	0.92
T	8	8	8	8	8	8	8	8	8	8
Alvi	0.05	0.7	0.9	0.08	0.07	0.08	0.1	0.19	0.6	0.86
Ti	0.13	0.10	0.11	0.13	0.13	0.14	0.11	0.14	0.14	0.144
Fe+3	0.28	0.38	0.48	0.47	0.40	0.46	0.40	0.33	0.36	0.40
Mg	3.46	3.29	3.29	3.25	3.37	3.28	3.34	3.27	3.34	3.34
Mn	0.043	0.049	0.44	0.42	0.039	0.037	0.039	0.034	0.037	0.036
Fe+2	1.02	1.09	0.97	1.002	0.985	0.980	0.960	1.105	1.14	0.049
Ca	0	0	0	0	0	0	0	0	0	0
C	5	5	5	5	5	5	5	5	5	5
Fe	0.08	0.08	0.05	0.03	0.06	0.034	0.076	0.00	0.062	0.064
Ca	1.78	1.74	1.74	1.77	1.76	1.76	1.74	1.78	1.78	1.74
Na	0.135	0.227	0.197	0.78	0.165	0.02	0.184	0.218	0.157	0.159
B	2	2	2	22	2	2	2	2	2	2
Ca	0	0	0	0	0	0	0	0	0	0
Na	0.23	0.17	0.16	0.16	0.195	0.206	0.133	0.205	0.272	0.206
K	0.101	0.118	0.094	0.088	0.057	0.65	0.060	0.139	0.096	0.87
Sum A	0.33	0.296	0.254	0.256	0.252	0.271	0.193	0.345	0368	0.348
Sum cations	15.33	15.29	15.25	15.25	15.25	15.27	15.19	15.34	15.36	15.36

Revista Geoaraguaia
ISSN:2236-9716
Barra do Garças – MT
v.10, n. esp. Geologia e
Pedologia p. 80-107. Dez-2020

Table 2. Results of microprobe mineralization in granodiorite based on 23 structural oxygen. Source: Kansaran Binaloud Institute of Iran.

GEOCHEMISTRY

Nomenclature of Sarduieh igneous rocks were accomplished based on the results of geochemical analysis. Geochemical characteristics of major and trace elements along with the petrographic observations can provide information on the origin and evolution of magma in igneous rocks. The content of trace and major elements in the rock samples are shown in Table 3.

Based on the Total Alkali-Silica (TAS) diagram after Middlemost (1994), which shows the relationships between the total alkali and the silica content, Sarduieh intrusive rocks can be classified as diorite, monzo-diorite, granodiorite and granite. According to the R1 versus R2 multicationic classification plot of De La Roche *et al.* (1980), the studied rock samples fall within diorite, tonalite, granodiorite and granite fields. (Figure 7).

The AFM diagram after Irvine and Baragar (1971) was used to describe the evolution of the parent magma and to differentiate the calc-alkaline and tholeiitic magmas, the two main subdivisions of the subalkaline magma series. According to this diagram, all of the rock samples plot in calc-alkaline field. Moreover, to determine the origin of magma and the influence of continental crust, aluminum saturation index diagram proposed by Shand (1947) was applied and showed that all of the samples are of metaluminous type. Based on the SiO_2 against K_2O diagram (Peccerillo, Taylor, 1976), the studied rocks fall within the calc-alkaline series.

The high ratios of A/CNK (= molar $Al_2O_3/CaO + Na_2O+K_2O$) and A/NK (= molar Al_2O_3/Na_2O+K_2O) indicate metaluminous to peraluminous compositions (Shand, 1947) (Figure 8). In order to differentiate I-type and A-type granites and I-type and S-type granites, Zr versus SiO_2 (Collins *et al.*, 1982) and Na_2O versus SiO_2 (Chappell, White, 2001) diagrams

were applied, respectively. The result showed that the granitoids of Sarduieh are I-type (Figure 7).

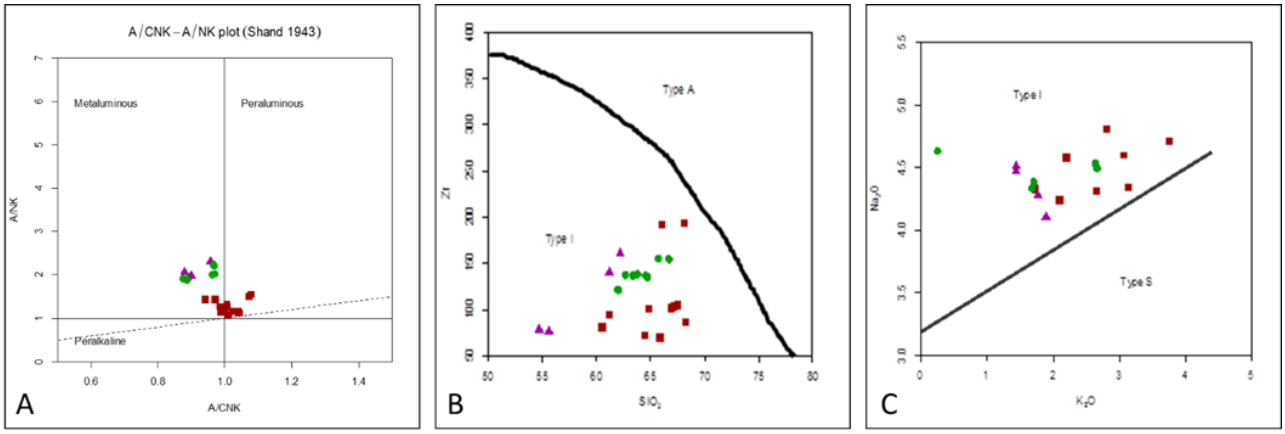

Figure 7. The location of the analyzed rock samples on (*a*) A/CNK vs. A/NK diagram; (*b*) Na_2O vs. K_2O diagram to discriminate I-type and S-type granites; (*c*) Zr vs. SiO_2 diagram to discriminate I-type and A-type granites.
Source: Shand (1947); Chappell and White (2001); Collins *et al.* (1982)

Variation of major and trace elements indicate the magmatic evolution processes such as fractional crystallization, partial melting, magmatic contamination and the affinity relations in rock suites (Harker 1896; Wilson, 2007). According to Harker diagrams, by increasing the concentration of SiO_2, the concentrations of CaO, Al_2O_3,TiO_2, MgO, Fe_2O_3 and P_2O_5 decrease and the values of K_2O and Na_2O_5 increase. This reveals the mafic composition of parent magma in the region (Raymond, 1995). Decreasing trend of MgO and FeO versus SiO_2 is related to the crystallization of mafic minerals such as magnetite, amphibole and biotite (Mason, Moore, 1982). Similarly, declining trend of TiO_2 content versus SiO_2 can be attributed to the presence of titanium-iron oxides in the rocks. The trends of CaO and Al_2O_3 with SiO_2 accords with differentiation of amphibole and calcic plagioclase phases and the trend of P2O5 with SiO_2 can be justified by the presence of apatite. Rising trend of K_2O and Na2O with SiO_2 can be ascribed to alkali-feldspar crystallization. Separation in diagrams is due to the alteration and lack of intermediate minerals.

Revista Geoaraguaia
ISSN:2236-9716
Barra do Garças – MT
v.10, n. esp. Geologia e
Pedologia p. 80-107. Dez-2020

According to Harker diagrams, with increasing in content of SiO_2 concentration of Th, Ba and Rb increases and concentration of Sr decreases. Ba and Rb due to substitution in K-bearing minerals such as orthoclase show an increasing trend toward the final stages of crystallization of magma. Thorium, due to its incompatibility and large ionic radius, remains in the liquid phase of a magma until the very last stages of crystallization and displays an increase in content with increasing in SiO_2 concentration and substitution of Sr for Ca in Ca-plagioclase lattice (Figure 8).

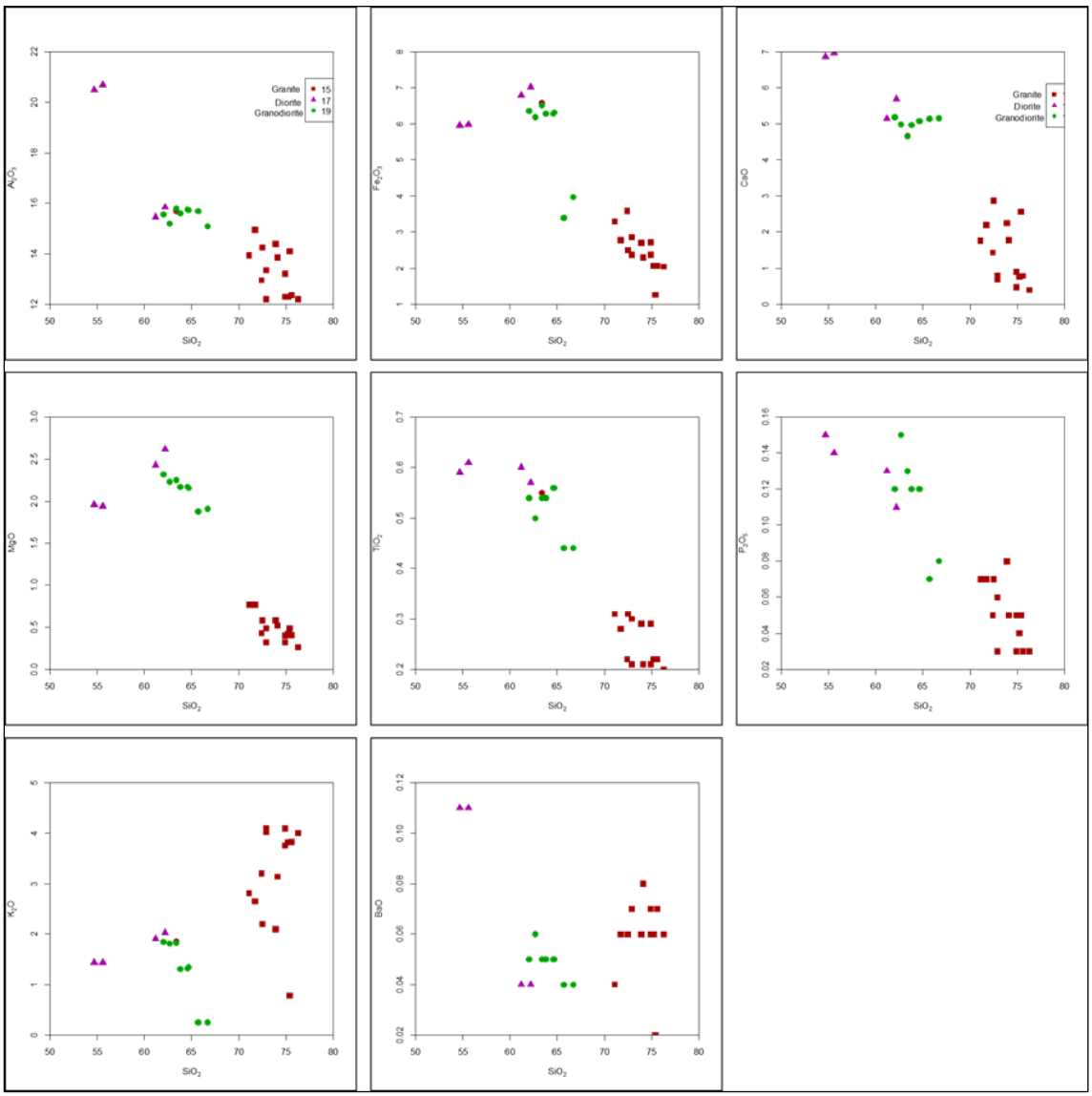

Figure 8. Variation diagrams of some major oxides against SiO_2.
Source: Harker (1896).

The results showed that the above-mentioned REEs and trace elements are incompatible during partial melting and fractional crystallization events and become dominant in the liquid phase throughout the differentiation (Stern, 2004). Chondrite-normalized REE (Nakamura, 1974) and Primitive mantle-normalized spider diagrams (McDonough, Sun, 1995) were applied to verify the changes in geochemical behavior of

Revista Geoaraguaia
ISSN:2236-9716
Barra do Garças – MT
v.10, n. esp. Geologia e
Pedologia p. 80-107. Dez-2020

elements . A decreasing parallel chondrite normalized REE pattern is found for all of the analyzed rocks (Nakamura, 1974).

This diagram shows that light rare earth elements (LREE) in the analyzed rocks are enriched compared to heavy rare earth elements (HREE) due to limited partial melting of mantle and remaining of garnet in the melt phase. Parallel trends to some extent indicate differentiation and fractional crystallization of minerals in the original magma. Both positive and negative Eu anomalies were observed showing the oxidizing and reducing conditions in the original magma (Kharbish, 2010). The negative Eu anomaly can be attributed to the plagioclase crystallization and reflects the formation of magma in a subduction zone (Kharbish, 2010).

According to the Primitive mantle-normalized spider diagrams (McDonough, Sun 1995), the studied igneous rocks are depleted from Ti, Nb, P and Ta and are enriched in Ce, Th, Ba, Zr, Sr and La. This characterizes the geochemical features of magmatic arcs in the subduction zone (Pearce *et al.*, 1990) and their relationship to the calc-alkaline series (Stern 2004). Spider diagrams display the high ratio of LREE/HREE and low ratio of HFSE/LILE which can be related to influence of the fluids or melts released from the subducting slab on the mantle wedge and its enrichment (Stern, 2004). These fluids are responsible for transferring incompatible elements from subducting crust to mantle wedge in magmatic arc region and its enrichment (Peng *et al.*, 2008).

The high partition coefficient of HFSEs in the remaining phases in the mantle (rutile and monazite) or separation of HFSE from the original mantle due to the former partial meting are among other factors contributing in depletion of HFSEs in the rocks from subduction zones (Stern, 2004) (Figure 9).

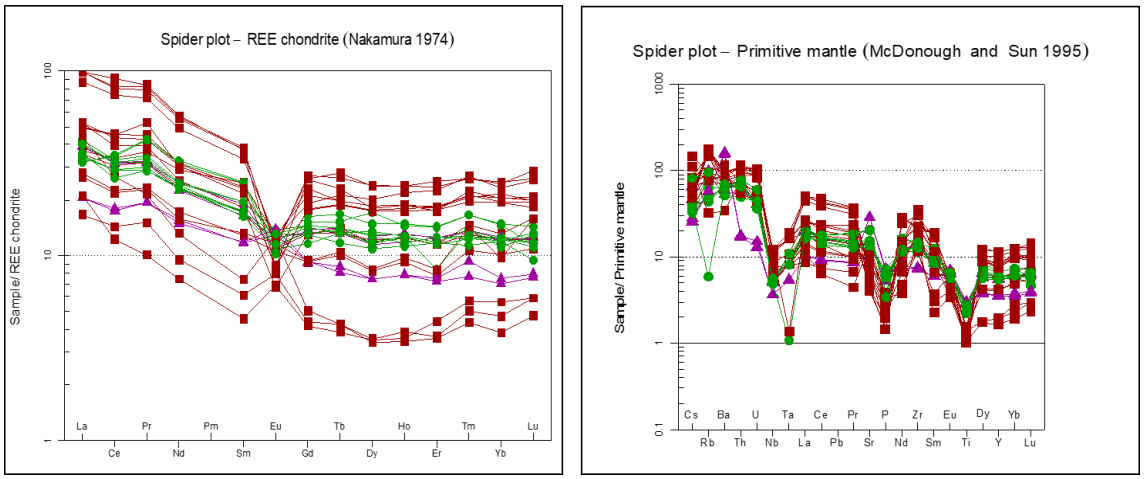

Figure 9. Chondrite-normalized REE and Primitive mantle-normalized spider diagrams. Source: Nakamura (1974); McDonough and Sun (1995).

The Rb versus Ta+ Yb and Nb versus Y diagrams (Pearce *et al.*, 1984) discriminate ORG and WPG, VAG + syn-COLG tectonic environment of granites. The studied granitoids plot in volcanic arc granitoid (VAG) field (Figure 12). The high content of Th in binary diagram of Th/Hf versus Ta/Hf Pearce)*et al.*, 1984) and Th versus Ta diagram (Schandl, Gorton, 2002) indicate that the rock samples locate in active continental margin field (Figure High .(12 ratios of Th in the Th/Hf versus Ta/Hf and Th versus Ta (Schandl, Gorton, 2002) diagrams show that the igneous rocks of the study area fall in the active continental margin field (Figure 10).

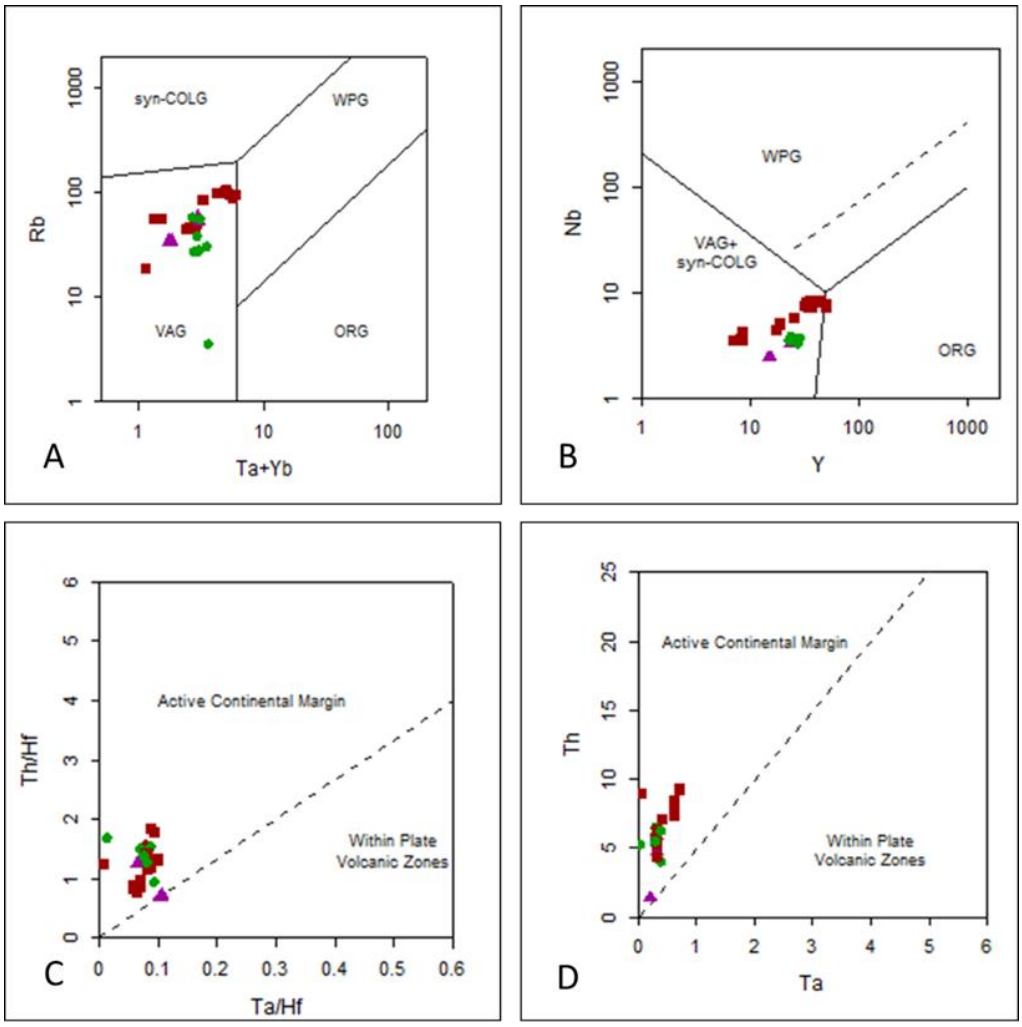

Figure 10. The position of the analyzed samples in tectono-magmatic discrimination diagrams; (*a*) Rb vs. Ta+ Yb; (*b*) Nb vs. Y; (*c*) Th/Hf vs. Ta/Hf; (*d*) Th vs. Ta.
Source: Pearce et al. (1984); Pearce et al. (1984); Schandl and Gorton (2002); Schandl and Gorton (2002).

Sample ID	LOI	SiO_2	Al_2O_3	Fe_2O_3	CaO	MgO	Na_2O	K_2O	Cr_2O_3	TiO_2	MnO	P_2O_5	SrO	BaO
E39	1.73	72.4	12.95	3.59	1.43	0.43	4.14	3.2	0.01	0.22	0.05	0.05	0.01	0.06
k2	1.35	62.2	15.85	7.03	5.7	2.62	3.32	2.03	0.01	0.57	0.13	0.11	0.03	0.04
k3	1.47	64.6	15.75	6.29	5.09	2.17	3.42	1.32	0.01	0.56	0.09	0.12	0.03	0.05
k4	0.67	72.5	14.25	2.5	2.87	0.58	4.58	2.2	0.01	0.31	0.02	0.07	0.03	0.06
S2	1.43	63.4	15.7	6.58	4.67	2.25	3.54	1.86	0.01	0.55	0.16	0.13	0.03	0.05
S3	0.96	62	15.55	6.36	5.2	2.32	3.6	1.85	0.01	0.54	0.13	0.12	0.03	0.05
S4	1.54	61.2	15.45	6.8	5.15	2.43	3.49	1.91	0.01	0.6	0.12	0.13	0.03	0.04

Sample ID	LOI	SiO_2	Al_2O_3	Fe_2O_3	CaO	MgO	Na_2O	K_2O	Cr_2O_3	TiO_2	MnO	P_2O_5	SrO	BaO
S5	0.9	72.9	13.35	2.86	0.69	0.49	4.34	4.09	0.01	0.3	0.06	0.06	0.02	0.07
S6	0.58	76.3	12.2	2.04	0.4	0.26	4.26	4	0.01	0.2	0.03	0.03	0.01	0.06
S7	0.7	74.9	13.2	2.72	0.47	0.4	4.71	3.76	0.01	0.29	0.05	0.05	0.01	0.06
S8	1.45	71.1	13.95	3.3	1.77	0.77	4.81	2.81	0.01	0.31	0.05	0.07	0.02	0.04
S9	0.67	74.9	12.3	2.38	0.9	0.32	3.89	4.09	0.01	0.21	0.03	0.03	0.02	0.07
S10	0.86	75.6	12.35	2.06	0.79	0.41	3.94	3.83	0.01	0.22	0.04	0.03	0.01	0.07
S11	1.38	63.8	15.6	6.29	4.97	2.17	3.44	1.31	0.01	0.54	0.03	0.12	0.03	0.05
S12	1.39	66.7	15.1	3.97	5.16	1.91	4.63	0.25	0.01	0.44	0.03	0.08	0.05	0.04
S13	2.03	54.7	20.5	5.96	6.87	1.96	4.47	1.44	0.01	0.59	0.11	0.15	0.07	0.11
S14	1.97	55.6	20.7	5.99	6.97	1.94	4.51	1.44	0.01	0.61	0.11	0.14	0.07	0.11
S15	1.02	75.4	14.1	1.26	2.57	0.49	5.47	0.78	0.01	0.22	0.04	0.05	0.03	0.02
S16	0.83	74.1	13.85	2.3	1.78	0.52	4.34	3.14	0.01	0.21	0.02	0.05	0.02	0.08
S17	0.96	71.7	14.95	2.78	2.2	0.77	4.31	2.65	0.01	0.28	0.02	0.07	0.03	0.06
S18	1.49	62.7	15.2	6.2	4.99	2.23	3.7	1.81	0.01	0.5	0.9	0.15	0.05	0.06
S19	0.59	73.9	14.38	2.7	2.25	0.58	4.24	2.1	0.01	0.29	0.02	0.08	0.02	0.06
S20	1.67	72.9	12.2	2.38	0.8	0.32	3.89	4.02	0.01	0.21	0.03	0.03	0.02	0.07
S21	1.47	64.7	15.74	6.32	5.09	2.16	3.4	1.34	0.01	0.56	0.09	0.12	0.03	0.05
S22	1.44	63.4	15.8	6.52	4.66	2.25	3.55	1.82	0.01	0.54	0.15	0.13	0.03	0.05
S23	1.38	65.7	15.7	3.39	5.14	1.88	4.63	0.25	0.01	0.44	0.03	0.07	0.04	0.04
S24	0.89	75.2	12.3	2.06	0.77	0.42	3.94	3.82	0.01	0.22	0.04	0.04	0.02	0.06

Table 3. The results of geochemical analysis ICP-MS of the rock samples (mg kg-1)
Source: ALS CAN CAD (2020).

Sample ID	Ba	Ce	Cr	Cs	Dy	Er	Eu	Ga	Gd	Hf	Ho	La	Lu	Nb
E39	507	34.1	10	1.48	4.01	2.58	0.52	13.1	3.61	5	0.87	17.4	0.54	5.6
k2	395	27.4	10	1.37	3.93	2.8	0.97	16.7	3.66	4.6	0.83	13	0.43	3.3
k3	444	28.5	10	0.85	4.46	2.82	1.06	17.3	4	3.8	0.91	13.9	0.4	3.6
k4	586	19.5	10	1.37	2.82	1.75	0.81	15	2.55	5.1	0.65	9.3	0.37	4.3
S2	462	26.7	10	0.76	4.14	2.57	0.84	16.5	3.61	3.8	0.88	11.7	0.42	3.4
S3	422	25.3	10	0.74	3.75	2.64	1.01	15.9	3.6	3.4	0.79	11.2	0.32	3.5
S4	348	27.6	10	0.98	4.35	2.8	0.85	15.8	3.82	3.6	0.92	12.9	0.41	3.5
S5	665	64.5	10	1.16	6.35	3.92	0.96	14.8	6.36	8.4	1.32	28.9	0.71	7.2
S6	544	79.2	9	0.93	6.2	4.13	0.66	14.1	7.15	6.9	1.31	32.8	0.68	7.8
S7	526	29.3	10	0.94	6.41	4.12	0.98	15.6	5.86	8.5	1.32	12.2	0.67	8
S8	407	37.7	10	1.73	6.89	5.08	0.94	16.3	5.32	9.1	1.54	17.4	0.87	8
S9	654	71.6	10	1.07	8.24	5.29	0.85	13.7	7.47	6.9	1.67	32.7	0.89	7.7
S10	634	39.4	10	1.14	6.04	4.1	0.66	12.6	4.91	7.2	1.26	16.4	0.66	7.1
S11	424	28.1	10	0.82	4.07	2.67	0.93	16.2	3.94	3.8	0.89	13.3	0.44	3.5

Sample ID	Ba	Ce	Cr	Cs	Dy	Er	Eu	Ga	Gd	Hf	Ho	La	Lu	Nb
S12	412	30.4	10	0.68	5.11	3.25	0.89	15.3	4.5	4.3	1.04	10.6	0.49	3.6
S13	1065	15.6	10	0.54	2.56	1.69	1	19	2.54	1.9	0.55	6.8	0.27	2.4
S14	1010	15.1	10	0.58	2.55	1.63	1.07	19.8	2.57	1.9	0.55	6.8	0.26	2.4
S15	227	12.4	10	2.32	1.16	0.8	0.61	13.2	1.21	3.4	0.24	5.5	0.16	3.4
S16	774	23.4	10	1.44	1.21	0.82	0.96	14.1	1.39	3.2	0.27	14.6	0.2	3.5
S17	563	10.6	10	3.07	1.2	0.99	0.53	14.2	1.15	3.7	0.25	7	0.2	4.1
S18	341	22.9	10	1.7	4.63	1.9	0.84	14.8	3.2	4.2	0.89	11.9	0.38	3.4
S19	579	18.9	10	1.36	2.88	1.89	0.89	14.9	2.59	5.1	0.68	8.78	0.54	4.9
S20	622	69.9	10	1.02	8.2	5.7	0.88	13.8	7.2	9.2	1.66	32.7	0.98	7.2
S21	444	27.5	10	0.79	4.38	2.83	1.01	17.4	4	3.9	0.82	13.2	0.4	3.7
S22	462	25.2	10	0.69	3.99	2.57	0.88	16.8	3.66	3.1	0.88	11.5	0.45	3.4
S23	412	29.9	10	0.78	5.9	3.22	0.79	15.9	4.2	4.9	1.02	10.7	0.39	3.2
S24	634	38.8	10	1.2	5.97	3.99	0.68	12.2	4.89	7.1	1.22	16.2	0.62	7.4

Table 4. The results of geochemical analysis ICP-MS of the rock samples (mg kg-1)
Source: ALS CAN CAD (2020).

Sample ID	Pr	Rb	Sm	Sn	Sr	Ta	Tb	Th	Tm	U	V	W	Y	Yb	Zr
E39	4.39	87.2	3.68	2	128	0.4	0.66	7.04	0.44	1.8	17	1	25	2.89	177
k2	3.55	59.1	3.35	1	274	0.3	0.62	5.8	0.4	1.1	175	6	23.6	2.64	161
k3	3.89	27.4	3.96	2	305	0.3	0.66	5.82	0.37	0.75	147	3	25.5	2.79	136
k4	2.61	46.7	2.62	2	220	0.3	0.47	4.56	0.32	0.91	38	1	17.3	2.24	203
S2	3.58	45.7	3.52	1	283	0.3	0.63	5.9	0.39	0.81	141	2	23.8	2.68	136
S3	3.37	37.9	3.48	1	280	0.3	0.55	5.18	0.34	0.71	144	1	22.9	2.63	121
S4	3.63	54.5	3.87	1	272	0.3	0.66	4.68	0.41	0.81	160	2	25.2	2.77	140
S5	8	107	6.81	2	132	0.6	0.93	8.38	0.67	1.64	16	1	35.6	4.49	312
S6	9.47	101.5	7.58	1	81	0.7	1.08	9.2	0.63	1.9	8	1	32.3	4.52	218

Sample ID	Pr	Rb	Sm	Sn	Sr	Ta	Tb	Th	Tm	U	V	W	Y	Yb	Zr
S7	4.09	96.1	5.04	1	107	0.6	0.93	7.59	0.62	1.77	15	1	35.1	4.79	314
S8	4.81	89.7	4.4	2	177.5	0.6	1	7.26	0.81	1.92	21	1	44.1	5.13	370
S9	9.19	97	7.79	1	141	0.6	1.24	8.38	0.78	1.96	9	1	49.6	5.5	233
S10	5.06	102.5	4.76	2	85.3	0.6	0.89	8.4	0.64	2.09	10	1	34	4.29	236
S11	3.59	26.6	3.46	2	290	0.3	0.62	5.49	0.42	0.76	145	3	24.3	2.45	138
S12	4.77	30.2	5.07	2	408	0.3	0.79	6.41	0.5	1.17	125	1	28.5	3.28	154
S13	2.18	34.7	2.39	1	575	0.2	0.41	1.41	0.28	0.3	74	1	15.3	1.65	78
S14	2.17	34.8	2.4	1	573	0.2	0.38	1.35	0.23	0.26	76	1	15	1.54	76
S15	1.69	19.2	1.24	1	268	0.3	0.2	6.32	0.13	0.88	30	1	7.1	0.84	123
S16	2.41	57.1	1.5	1	190	0.3	0.2	5.72	0.15	1.13	27	1	8.2	1.03	120
S17	1.13	57.5	0.92	1	273	0.3	0.18	5.26	0.17	1.17	42	1	8.3	1.23	164
S18	3.23	54.3	3.29	1	252	0.4	0.62	3.98	0.41	0.87	158	2	25.7	2.7	137
S19	2.55	45.9	2.68	2	210	0.3	0.49	4.34	0.43	0.88	32	1	18.3	2.12	201
S20	8.9	97	7.7	1	139	0.6	1.32	8.34	0.78	1.92	9	1	49.7	5.4	232
S21	3.78	28.5	3.97	2	307	0.3	0.66	5.4	0.38	0.75	147	2	24.5	2.71	135
S22	3.23	57	3.55	1	281	0.04	0.64	5.2	0.37	0.89	141	2	23.8	2.66	136
S23	4.72	3.5	5.05	2	402	0.4	0.72	6.23	0.5	1.2	122	1	28.2	3.24	155
S24	5.9	101.1	4.66	1.5	85.1	0.05	0.88	8.9	0.59	2.08	10	1	32	4.26	234

Table 5. The results of geochemical analysis ICP-MS of the rock samples (mg kg-1)

Source: ALS CAN CAD (2020).

CONCLUSION

Granitoid rocks of north of Sarduieh with the age of Oligo-Miocene are located in Urumieh-Dokhtar Magmatic Arc and range in composition from diorite to granite.

Geochemical studies showed that the amphibole minerals in diorite and granodiorites are calcic in composition and range from actinolite to magnesio-hornblende. Geochemical and mineralogical results revealed that these bodies have been generated in

the lower part of the lower crust at a temperature of 700 to 750 °C, with an oxygen fugacity of -13.57 to -15.76 and a low pressure of 1 to 3 kb .Geochemical study revealed that the original magma has been high-K, calc-alkaline metaluminous and display I-type affinities. These rocks are enriched in LILE (e.g. Ba, Rb, Th) and depleted from HFSE (e.g. Ti, P, Nb) which reflect the characteristics of subduction and active continental margin environments. The variation trends of major oxides and trace elements against SiO2 and the presence of plagioclase, alkali-feldspar, quartz and biotite show that fractional crystallization has played a pivotal role in evolution of Sarduieh igneous rocks. This study showed that the granitoids of Sarduieh fall in the volcanic-arc granite (VAG) field. Moreover, considering the situation of the study area in Urumieh-Dokhtar Magmatic Arc, it is suggested that Sarduieh igneous rocks were generated as a result of Neotethys subduction beneath the Central Iranian plate.

REFERENCES

AFTABI, A.; ATAPOUR, H. Regional aspects of shoshonitic volcanism in Iran, **Episodes**, 23, 2000. p. 119-125.

AGARD, P.; OMRANI, J.; JOLIVET, L.; MOUTHEREAU, F. Convergence history across Zagros (Iran): constraints from collisional and earlier deformation. **International Journal of Earth Sciences**, n. 94, 2005. p. 401-419.

AGARD, P. *et al.*, Zagros orogeny: a subduction-dominated process. **Geological Magazine**, 148, 2011. p. 692-725

ALAVI, M. Tectonics of the Zagros orogenic belt of Iran: new data and interpretations. **Tectonophysics**, n. 229, 1994. p. 211-238.

ALLEN, M.; JACKSON J.; WALKER, R**. Late Cenozoic reorganization of the Arabia-Eurasia collision and the comparison of shor-term and long-term deformation rates**. Tectonics 23‹ TC2008‹ doi:10.1029/2003TC001530‹ 16 pp.
AMIDI, S. Étude géologique de la région de Natanz-Surk (Iran, Central), **Geological Survey of Iran**. Thèse Ph.D.‹ Univ. Grénoble‹ France‹ 316pp.

ANDERSON, J. L.; SMITH, D. R. The effects of temperature and fogasite on the Al-in-hornblende barometer. **American Mineralogist**, 80, 1995. p. 549-559.

BACON, C. R.; DRUITT, T. H. Compositional evolution of the zoned calcalkaline magma chamber of Mount Mazama, Crater Lake, Oregon, **Contributions to Mineralogy and Petrology**, n. 98, 1988. p. 224-256.

BERBERIAN, M.; KING, G. Towards a paleogeography and tectonic evolution of Iran. **Canadian journal of earth sciences**, 18, 1981, p. 210-265.

BERBERIAN, F.; MUIR, I.; PANKHURST, R.; BERBERIAN, M. Late Cretaceous and early Miocene Andean-type plutonic activity in northern Makran and Central Iran. **Journal of the Geological Society**, n. 139, 1982. p. 605-614.

BULLEN, T. D.; CLYNNE, M. A. Trace element and isotopic constraints on magmatic evolution at Lassen volcanic center. **Journal of Geophysical Research: Solid Earth**, n. 95, 1990. p. 19671-19691.

CELIC, O. F.; DELALOYE, M. F. Characteristics of ophiolite related metamorphic rocks in the Beysehir ophiolitic mélange (central taurides, Turkey), Deduced from whole rock and mineral chemistry. **Journal of Asian Earth Science**, 26, 2006. p. 452-476.

COLTORTI, M. C.; BONADIMAN, B.; FACCINI, M.; GRÉGOIRE, S. Y.; O'REILLY W.; POWELL, W. Amphiboles from suprasubduction and intraplate lithospheric mantle. **Lithos**, n. 99, 2007. p. 68-84.

DEWEY, J.; HELMAN, M.; KNOTT, S.; TURCO, E.; HUTTON, D. Kinematics of the western Mediterranean. **Geological Society, London, Special Publications**, 45, 1989. p. 265-283

DILEK, Y.; ALTUNKAYNAK, Ş.; ÖNER, Z. Syn-extensional granitoids in the Menderes core complex and the late Cenozoic extensional tectonics of the Aegean province. **Geological Society, London, Special Publications**, 321, 2009. p. 197-223.

DILEK, Y.; IMAMVERDIYEV, N.; ALTUNKAYNAK, Ş. Geochemistry and tectonics of Cenozoic volcanism in the Lesser Caucasus (Azerbaijan) and the peri-Arabian region: collision-induced mantle dynamics and its magmatic fingerprint. **International Geology Review**, 52, 2010. p. 536-578.

DILEK, Y.; SANDVOL, E. Seismic structure, crustal architecture and tectonic evolution of the Anatolian-African plate boundary and the Cenozoic orogenic belts in the Eastern Mediterranean region. **Geological Society, London, Special Publications**, n. 327, 2009. p. 127-160.

DE LA ROCHE, H.; LETERRIER, J. T.; GRANDCLAUDE, P.; MARCHAL, M. A classification of volcanic and plutonic rocks using R1R2-diagram and major-element analyses—its relationships with current nomenclature. **Chemical Geology**, 29, 1980. p. 183-210

EMAMI, M. H. **Géologie de la région de Qom-Aran (Iran)**: Contribution a l'étude dynamique et géochimique du volcanisme Tertiaire de l'Iran Central, Ph.D. thesis, France, University of Grenoble, France, 1981. 489 p.

GHASEMI, A.; TALBOT, C. J. A. New tectonic scenario for the Sanandaj–Sirjan Zone (Iran). **Journal of Asian Earth Sciences**, 26, 2006. p. 683-693

GIRET, A.; BONIN, B.; LEGER, J. M. Amphibole compositional trends in oversaturated and undersaturated alkaline plutonic ring-composition. **The Canadian Mineralogist**, 18(4), 1980. p. 481-495.

GROVE, T.; DONNELLY-NOLAN, J. The evolution of young silicic lavas at Medicine Lake Volcano, California: Implications for the origin of compositional gaps in calc-alkaline series lavas. **Contributions to Mineralogy and Petrology**, 92, 1986. p. 281-302

GSI, **1:100000 geological map of Sarduiyeh**. Geological Survey of Iran: Tehran, 1972.

GUFFANTI, M.; CLYNNE, M. A.; MUFFLER, L. P. Thermal and mass implications of magmatic evolution in the Lassen volcanic region, California, and minimum constraints on basalt influx to the lower crust, **Journal of Geophysical Research: Solid Earth**, n. 101, 1996. p. 3003-3013.

HAMMARSTROM, J. M.; ZEN, E. Aluminum in hornblende: An empirical igneous geobarometer. **American Mineralogist**, 71, 1986. p. 1297-1313.

HARKER, A. **The natural history of igneous rocks**. Methuen: London, 1909.

HELZ, R. T. Phase relations of basalts in their melting ranges at P H2O= 5 kb. Part II. Melt compositions. **Journal of Petrology**, 17, 1976. p. 139-193.

HOLLISTER, L. S.; GRISSOM, G. C.; PETERS, E. K.; STOWELL, H. H.; SISSON, V. B. Confirmation of the empirical correlation of Al in hornblende with pressure of solidification of clac-alkaline plutons. **American Mineralogist**, 72, 1987. p. 231-239.

IRVINE, T.; BARAGAR, W. A guide to the chemical classification of the common volcanic rocks, **Canadian Journal of Earth Sciences**, n. 8, 1971, p. 523-548.

KARIG, D. E. Origin and development of marginal basins in the western Pacific. **Journal of geophysical research**, 76, 1971. p. 2542-2561.

JOHNSON, M. C.; RUTHERFORD, M. J. **Experimental calibration of the aluminum-in-hornblende geobarometer with applications to Long Valley Caldera (California) volcanic rocks**. **Geology**, 17, 1989. p. 837-841.

KHARBISH, S. Geochemistry and magmatic setting of Wadi El-Markh island-arc gabbro–diorite suite, central Eastern Desert, Egypt. Chemie der Erde-Geochemistry, n. 70, 2010. p. 257-266.

LEAKE, B. E.; WOOLLEY, A. R.; ARPS, C. E.; BIRCH, W. D.; GILBERT, J. M. C.; GRICE, J. D.; HAWTHORNE, F. C.; KATO, A.; KISCH, H. J.; KRIVOVICHEV, V. G. Report. Nomenclature of amphiboles: report of the subcommittee on amphiboles of the international mineralogical

association commission on new minerals and mineral names. **Mineralogical magazine**, 61, 1997. p. 295-321.

LESCUYER, J. L.; RIOU, R. **Géologie de la région de Mianeh (Azerbaijan): contribution à l'étude du volcanisme tertiaire de l'Iran**. Université Scientifique et Médicale de Grenoble: Grenoble, 1976.

MASON, B.; MOORE, C. B. **Principles of geochemistry**. John Wiley and Sons,New York, 1982.

MCDONOUGH, W. F.; SUN, S. S. The composition of the Earth. **Chemical Geology**, n. 120, 1995. p. 223-253.

MIDDLEMOST, E. A. Naming materials in the magma/igneous rock system. **Earth-Science Reviews**, 37, 1994. p. 215-224

MCCLUSKY, S.; BALASSANIAN, S.; BARKA, A.; DEMIR, C.; ERGINTAV, S.; GEORGIEV, G.; GURKAN, O.; HAMBURGER, M.; HURST, K.; KAHLE, H.; KASTENS, K.; KEKELIDZE, G.; KING, R.; KOTZEV, V.; LENK, O.; "**Global Positioning System constraints on plate kinematics and dynamics in the eastern Mediterranean and Caucasus**", Journal of Geophysical Research 105 (2000) 5695–5719.

MOÏNE-VAZIRI, H. **Volcanisme tertiaire et quaternaire en Iran**, These d'Etat. Univers. Paris-Sud ‹Orsay, éditeur inconnu, 1985.

MOLINA, J.; SCARROW, J.; MONTERO, P. G.; BEA, F. High-Ti amphibole as a petrogenetic indicator of magma chemistry: evidence for mildly alkalichybrid melts during evolution of Variscan basic–ultrabasic magmatism of Central Iberia. **Contribution to Mineralogy and Petrology**, n. 158, 2009. p. 69-98.

NAKAMURA, N. Determination of REE, Ba, Fe, Mg, Na and K in carbonaceous and ordinary chondrites. **Geochimica et Cosmochimica Acta**, 38, 1974. p. 757-775

NICKEL, E. H.; ROCK, N. M. S.; SCHMUCHER, J. C.; SMITH, D. C.; STEPHENSON, N. C. N.; UNUNGARETTI, L.; WHITTAKER, E. J. W.; YOUZHI, G. Nomenclature of Amphiboles, Report of the Subcommittee on Amphiboles of the International Mineralogical Association Commission on New Minerals Names. **Europian Journal of Mineralogy**, 9, 1997. p. 623-651.

NOWROOZI, A. A. Seismo-tectonics of the Persian plateau, eastern Turkey, Caucasus, and Hindu-Kush regions. **Bulletin of the Seismological Society of America**, 61, 1971. p. 317-341.

PEARCE, J. *et al.* Genesis of collision volcanism in Eastern Anatolia, Turkey, Journal of Volcanology and Geothermal Research, 44, 1990. p. 189-229.

PEARCE, J. A.; HARRIS, N. B.; TINDLE, A. G. Trace element discrimination diagrams for the tectonic interpretation of granitic rocks. **Journal of Petrology**, 25, 1984. p. 956-983.

PECCERILLO, A.; TAYLOR, S. Geochemistry of Eocene calc-alkaline volcanic rocks from the Kastamonu area, northern Turkey. **Contributions to Mineralogy and Petrology**, 58, 1976. p. 63-81

PENG, T.; WANG, Y.; ZHAO, G.; FAN, W.; PENG, B. Arc-like volcanic rocks from the southern Lancangjiang zone, SW China: geochronological and geochemical constraints on their petrogenesis and tectonic implications. **Lithos**, n. 102, 2008. p. 358-373.

RASOULI, J.; GHORBANI, M.; AHADNEJAD, V. Field observations, Petrography and microstructures study of Jebale Barez Plutonic complex (East-North East Jiroft). **Journal of Tethys**, Vol 2, 2014. p. 178-195.

RAYMOND, L. A. **Petrology: the study of igneous, sedimentary**. Metamorphic rocks, vol 3. Wm. C. Brown Dubuque: Iowa, 1995.

ROBERTS, M. P.; CLEMENS, J. D. Origin of high-potassium, calc-alkaline, I-type granitoids, **Geology**, 21, 1993. p. 825-828.

SABZEHEI, M. **Geological Quadrangle Map of Iran**, No. 12, Hajiabad, 1:250,000, First compilation by BERBERIAN, M., final compilation and revision by SABZEHEI, M., Geological Survey of Iran, 1994.

TAKIN, M. **Iranian geology and continental drift in the Middle East**, . Nature 235 : 147-150,1972.

TEPPER, J. H.; NELSON, B. K.; BERGANTZ, G. W.; IRVING, A. J. Petrology of the Chilliwack batholith, North Cascades, Washington: generation of calc-alkaline granitoids by melting of mafic lower crust with variable water fugacity. **Contributions to Mineralogy and Petrology**, n. 113, 1993. p. 333-351.

SCHMIDT, M. W. Amphibole composition in tonalite as a function of pressure: an experimental calibration of the Al-in hornblende barometer. **Contribution Mineralogy and Petrology**, 110, 1992. p. 304-305.

SIAL, A. N.; FERREIRA, V. P.; FALLICK, A. E.; CRUZ, M. J. M. Amphibole-rich clots in calc-alkalic granitoids in the Borborema province, northeastern Brazil. **Journal of South American Earth Sciences**, 11, 1998. p. 457-471.

SCHANDL, E. S.; GORTON, M. P. Application of high field strength elements to discriminate tectonic settings in VMS environments. **Economic Geology**, 97, 2002. p. 629-642.

SHAND, S. J. Eruptive rocks: their genesis, composition, classification, and their relation to ore-deposits, with a chapter on meteorites. New York: John Wiley & Sons.
Shand، S.Y.،1947، the study of rocks، London thomas. Marby and Co. P. 236.

STERN, R. J. Subduction initiation: spontaneous and induced. **Earth and Planetary Science Letters**, 226, 2004. p. 275-292

VYHNAL, C. R.; MCSWEEN, H. Y.; SPEER, J. A. Hornblende Chemistry in Southern Appalachian Granitoids: implications for aluminum hornblende thermo barometry and magmatic epidote stability. **American Mineralogist**,76, 1991. p. 176-188.

WILSON, B. M. **Igneous petrogenesis a global tectonic approach**. Springer Science & Business Media and ancient marginal basins: Geological Society of London Special , 27 mars **2007**

WONES, D. R. Significance of the assemblage titanite +magnetitet +quartze in granitic rocks. **American Mineralogist**, 74, 1989. p. 744-749.